Acoustic propagation in 3-D, rectangular ducts with flexible walls

Jane B. Lawrie[a)]
Department of Mathematics
Brunel University, Uxbridge
UB8 3PH, UK

Abstract
In this article some analytic expressions for acoustic propagation in 3-D ducts of rectangular cross-section and with flexible walls are explored. Consideration is first given to the propagation of sound in an unlined 3-D duct formed by three rigid walls and closed by a thin elastic plate. An exact closed form expression for the fluid-structure coupled waves is presented. The effect of incorporating internal structures, such as a porous lining, into the duct is also discussed. Such configurations are directly relevant to the heating, ventilation and air-conditioning industry.

1 Introduction

Heating, ventilation and air-conditioning (HVAC) ducts form an intrinsic feature of many buildings, aircraft and other engineering structures. The presence of such ducts is clearly beneficial, but they are also a channel for unwanted noise. Sound from fans and/or motors can propagate for significant distances along ducting systems, and the issue of noise control has long been of interest to scientists and engineers. There are two major mechanisms by which sound travels along ducts: by reflection from the internal walls and as vibration along the wall itself. Traditional analytic methods for modelling sound propagation in 3-D ducts have tended to neglect the latter, primarily because the exact form of the propagating waves was unknown.

Recent research, [5], has established both the analytic waveforms and many of their mathematical properties. This prepares the ground for the development of full hybrid analytic/numerical solutions to model problems directly related to the noise control issues described above. These recent advances are discussed in this paper. It is shown that the theory is applicable to a wide class of 3-D ducts, including configurations with both flexible walls and an internal layer of porous material.

[a)] Email address: Jane.Lawrie@brunel.ac.uk

A pre-requisite to formulating the waveforms for the unlined 3-D duct is an appreciation of wave propagation in the underlying 2-D duct, this is considered in section 2. The eigenfunctions for the 3-D case are stated in section 3. Of particular interest is the characteristic equation which defines the admissible wavenumbers. The properties of this equation and its roots are explored. An alternative representation for the 3-D eigenfunctions is given in section 4. In section 5 the theory is extended to other duct configurations, for example, those with a porous lining or internal membrane, [3]. Some concluding remarks are presented in section 6.

Throughout harmonic time dependence, $\exp(-i\omega t)$, is assumed. The full velocity potential is, thus, expressed in terms of the reduced potential by $\Phi(x, y, z, t) = \phi(x, y, z)\exp(-i\omega t)$. Furthermore, only symmetric waveforms are considered, that is, those for which $\phi(x, y, -z) = \phi(x, y, z)$. For the sake of brevity, the boundary value problems are not explicitly formulated, but rather stated in words. It is assumed, however, that they are non-dimensionalised with respect to time scale ω and length scale k where $k = \omega / c$ and c is the fluid sound speed.

2 The 2-D case

Before considering the 3-D duct, it is necessary to review wave propagation in the underlying 2-D system. The appropriate 2-D duct lies in the region $0 \le y \le a$, $-\infty < x < \infty$ of a non-dimensional Cartesian frame reference. The upper boundary comprises an elastic plate whilst the base, lying along $y = 0$, is rigid. The velocity potential satisfies Helmhlotz's equation and the elastic plate satisfies the usual thin plate equation, [6].

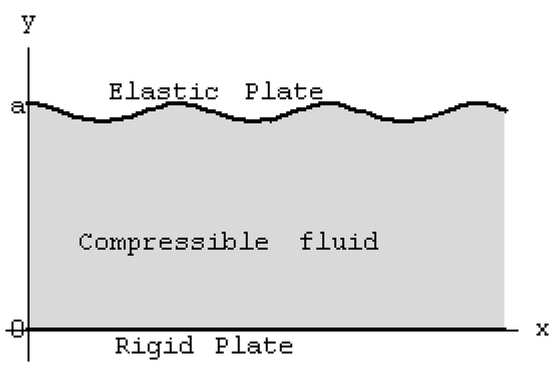

Figure 1: The 2-D duct comprising the xy-cross-section of the unlined 3-D case.

The velocity potential representing fluid-structural waves propagating in the positive x-direction has the form:

$$\phi(x,y) = \sum_{m=0}^{\infty} A_m Y_m(y) e^{i\zeta_m x}, \quad x > 0 \tag{1}$$

where $Y_m(y) = \cosh(\gamma_m y)$, A_m is the modal amplitude, $\zeta_m = \sqrt{\gamma_m^2 + 1}$ and is defined to be positive real or have positive imaginary part. The eigenvalues γ_m, $m = 0,1,2,\ldots$ are the roots of $K(\gamma) = 0$ where

$$K(\gamma) = ((\gamma^2 + 1)^2 - \mu^4)\gamma \sinh(\gamma a) - \alpha \cosh(\gamma a). \tag{2}$$

Here μ is the in vacuo plate wavenumber and α a fluid loading parameter. Thus,

$$\mu^4 = \frac{12(1-\nu^2)c^2\rho_p}{k^2h^2E}, \quad \alpha = \frac{12(1-\nu^2)c^2\rho_a}{k^3h^3E} \tag{3}$$

where E is Young's modulus, ρ_p is the density of the plate, ρ_a is the density of the compressible fluid and ν is Poisson's ratio. The eigenfunctions $Y_m(y)$, $m = 0,1,2,\ldots$ are linearly dependent (a feature that plays a key role in the construction of the 3-D duct modes) and satisfy the orthogonality relation

$$\alpha \int_0^a Y_m Y_j \, dy = C_m \delta_{mj} - (\gamma_j^2 + \gamma_m^2 + 2) Y_m'(a) Y_j'(a) \tag{4}$$

where the prime, here and throughout, indicates differentiation with respect to *y*, δ_{mj} is the usual Kronecker delta and C_m is given by

$$C_m = \frac{Y_m'(a)}{2\gamma_m} \frac{d}{d\gamma} K(\gamma) \bigg|_{\gamma=\gamma_m}. \tag{5}$$

Full details of this eigen-system are given by Lawrie, [6].

3 The unlined 3-D duct

Consideration is now given to the propagation of sound in an unlined 3-D duct formed by three rigid walls, lying along $y = 0$, $-b \le z \le b$, $-\infty < x < \infty$ and $z = \pm b$, $0 \le y \le a$, $-\infty < x < \infty$ and closed by a thin elastic plate lying along $y = a, -b \le z \le b$, $-\infty < x < \infty$. The elastic plate is assumed to be clamped to the rigid duct walls. That is, the plate displacement and gradient are both zero along the edges $y = a$, $z = \pm b, -\infty < x < \infty$.

As in the 2-D case, it is assumed that the fluid-structure coupled waves propagate in the positive x direction. Thus, the velocity potential has the form

$$\phi(x,y,z) = \sum_{n=0}^{\infty} B_n \psi_n(y,z) e^{is_n x}, \quad x > 0 \tag{6}$$

where $\psi_n(y,z)$, $n=0,1,2,\ldots$ are an infinite set of non-separable eigenfunctions, s_n are the

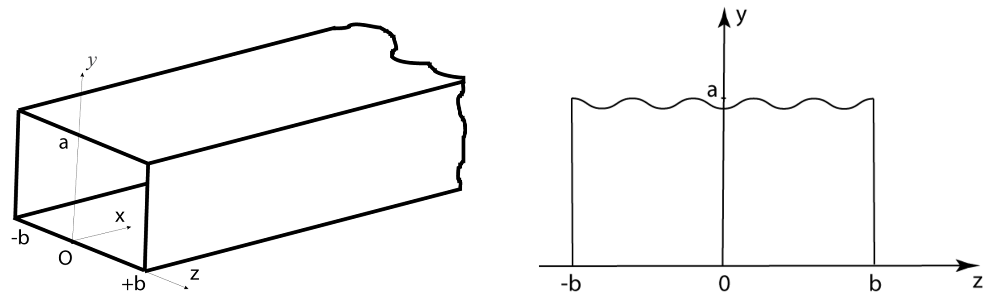

Figure 2: The unlined 3-D duct and its cross-section in the yz-plane.

admissible (non-dimensional) wavenumbers and B_n the wave amplitudes. The exact, closed form expression for the symmetric eigenfunctions, [6], is stated here as

$$\psi_n(y,z) = \sum_{m=0}^{\infty} \frac{Y_m'(a) Y_m(y) \cosh(\tau_{nm} z)}{C_m \tau_{nm} \sinh(\tau_{nm} b)}. \tag{7}$$

Here $Y_m(y)$ are the eigenfunctions for the underlying 2-D system discussed in section 2 and $\tau_{mn}^2 + \gamma_m^2 + 1 - s_n^2 = 0$. The admissible wavenumbers, $s_n, n=0,1,2,\ldots$, for the 3-D duct are given by $L(s)=0$ where

$$L(s) = \sum_{m=0}^{\infty} \frac{[Y_m'(a)]^2 \cosh[(s^2 - 1 - \gamma_m^2)^{1/2} b]}{C_m (s^2 - 1 - \gamma_m^2)^{1/2} \sinh[(s^2 - 1 - \gamma_m^2)^{1/2} b]}. \tag{8}$$

This characteristic equation is of an unusual form, being the sum over the eigenvalues for the underlying 2-D system, and it exhibits an infinite number of asymptotes. It is, however, a straightforward procedure to numerically solve (8). The roots have the following properties:

(i) for every root, s_n, there is another root, $-s_n$;

(ii) there is a finite number of real roots;

(iii) there is an infinite number of imaginary roots;

(iv) there is an infinite number of roots with non-zero real and imaginary parts.

In order that (6) represents only waves that travel in the positive x direction and/or decay exponentially as $x \to \infty$, the convention is adopted that the $+s_n$ roots are either positive real or have positive imaginary part. They are ordered sequentially, real roots first and then by increasing imaginary part. Thus, s_0 is always the largest real root. For any complex root, say

s_c, lying in the upper half of the complex s-plane, then minus the complex conjugate, $-s_c^*$, also lies in this half plane. Such pairs of roots are numbered according to the magnitude of their imaginary part, and in the order s_c followed by $-s_c^*$. Finally, it is assumed that $s_n \neq 0$ and that no root is repeated.

The above features are demonstrated in figures 3 and 4. In order that a useful comparison can be made, the physical parameters are the same as those chosen by Martin et al, [9]. Thus, the dimensional ducts height and width are respectively 0.09m and 0.106m, whilst the elastic plate comprises a sheet of aluminium, of thickness 0.0006m.

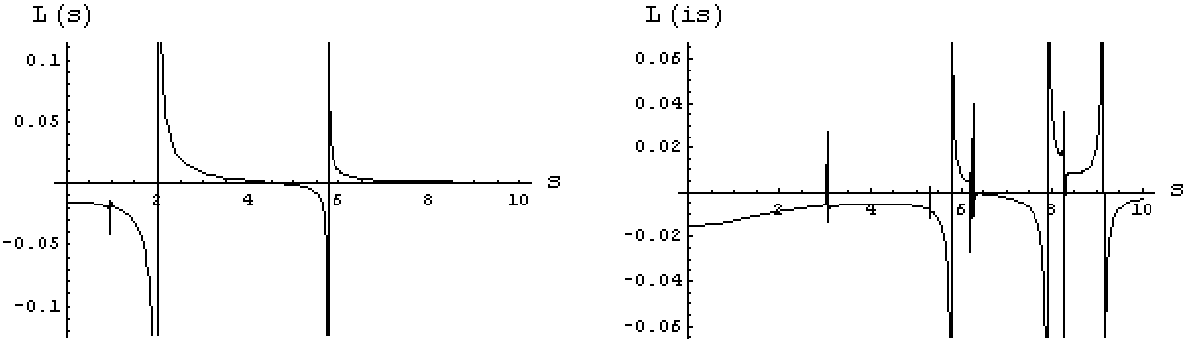

Figure 3: The dispersion relation for the unlined 3-D duct plotted for real and imaginary arguments at 600 Hz.

Figure 3 shows $L(s)$ plotted for real and imaginary arguments. The asymptotes are apparent and it can also be seen that the roots of $L(s)=0$ often lie very close to an asymptote. The rapid change of gradient in the close proximity of the roots can present problems for root finding algorithms such as the Newton-Raphson method. This situation is, however, improved by seeking the roots of $M(s)=0$ as opposed to $L(s)=0$ where

$$M(s) = L(s)\left\{\sum_{m=0}^{\infty}\frac{1}{C_m(s^2-1-\gamma_m^2)^{1/2}\sinh[(s^2-1-\gamma_m^2)^{1/2}b]}\right\}^{-1} . \tag{9}$$

Figure 4 shows the phase speeds for the frequency range 0-1500 Hz. This graph is in excellent agreement with that presented by Martin et al, [9], who used the Rayleigh-Ritz method. Also shown in figure 4, is the location in the complex s-plane of the roots $L(s)=0$ at a frequency of 600Hz. There are two real roots, an infinite number of imaginary roots and also an infinite family of complex roots. The latter lie on curves that are reminiscent of the parabolic arcs seen for propagation in a 2-D elastic slab, [1]. The eigenfunction method, although employed on a small duct herein, works equally well for larger ducts, [6].

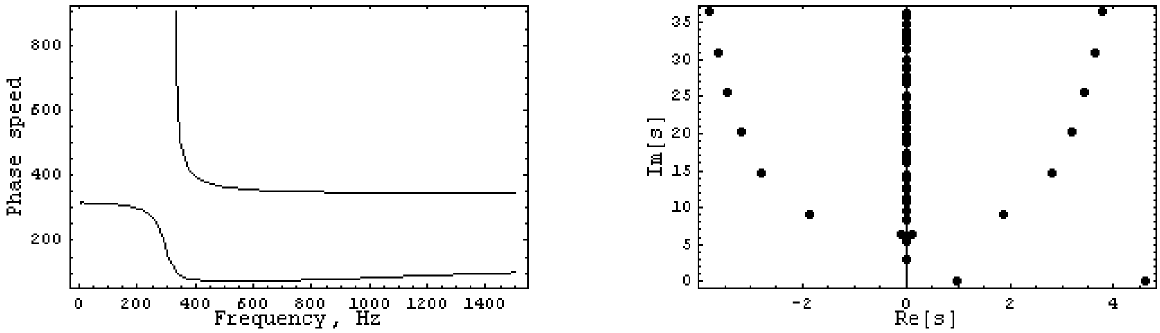

Figure 4: The phase speeds of the unattenuated waves plotted against frequency and the distribution of the roots in the complex s-plane at a frequency of 600Hz.

4 An alternative form for the duct modes

In section 3 the duct modes were expressed as a sum over the roots of the characteristic equation for the underlying 2-D eigensystem. Here an alternative representation is presented in which the 3-D duct modes are expressed as a Fourier cosine series in which the summation is over the values $m\pi / b, m = 0,1,2,\ldots$.

There are two approaches by which this can be done. The first approach is the method outlined in Lawrie and Kirby, [8]. This relates the two series through an integral in which both families of eigenvalues occur as poles. The appropriate integral is

$$I(s) = \lim_{X\to\infty} \int_{-X}^{X} \frac{\gamma \cosh(\gamma y)\cosh[(s^2-\gamma^2-1)^{1/2} z]\, d\gamma}{K(\gamma)(s^2-\gamma^2-1)^{1/2} \sinh[(s^2-\gamma^2-1)^{1/2} b]} = 0, \tag{10}$$

where $0 \le y \le a$, $0 \le z \le b$. The reader is referred to Lawrie and Kirby[8] for further details.

The alternative approach is to solve the full boundary value problem for the 3-D duct modes using a Fourier cosine series formulation. Note, however, that if this method is adopted it is necessary to modify the usual thin plate equation by equating it to a Delta function, $\delta(z-b)$.

It is found that

$$\psi_n(y,z) = \frac{2}{b}\sum_{m=0}^{\infty} \frac{(-1)^m \cosh[(s_n^2 - 1 + m^2\pi^2/b^2)^{1/2} y]\cos(m\pi z/b)}{\varepsilon_m K[(s_n^2 - 1 + m^2\pi^2/b^2)^{1/2}]} \tag{11}$$

where $\varepsilon_m = 2$ if $m=0$ and 1 otherwise. The characteristic function likewise can be expressed as

$$L(s) = \frac{2}{b}\sum_{m=0}^{\infty}\frac{(s^2-1+m^2\pi^2/b^2)^{1/2}\sinh[(s^2-1+m^2\pi^2/b^2)^{1/2}a]}{\varepsilon_m K[(s^2-1+m^2\pi^2/b^2)^{1/2}]}. \tag{12}$$

Both representations for $\psi_n(y,z)$ and $L(s)$ converge well, but expressions (11) and (12) have the advantage that the summation takes place across eigenvalues which can be stated explicitly.

5 Extension of the method

In sections 2-4 analytic representations for the travelling waves in a 3-D duct with one flexible wall have been constructed and discussed. Two representations have been presented, both of which take the form of an infinite sum but across different sets of eigenvalues. In section 3 the eigenmodes are constructed as a summation over γ_m, $m = 0,1,2,\dots$, that is, the roots of the dispersion relation for the 2-D duct shown in figure 1, and must be found numerically. In section 4 the waveforms are recast in a form whereby the summation is over $m\pi/b, m = 0,1,2,\dots$. The latter formulation is attractive in that the summation occurs over integer values. Although computationally more cumbersome, the formulation given in section 3 does, however, offer an advantage. Because it is expressed in terms of the eigenfunctions for xy-crossectional sub-system, it is a straightforward procedure to extend the theory to other 3-D duct configurations. In fact, the correct eigenfunction and characteristic equation for a wide class of 3-D ducts can be obtained from (7) and (8) simply by replacing $Y_m(y)$ and C_m with new expressions that are appropriate for the underlying 2-D system.

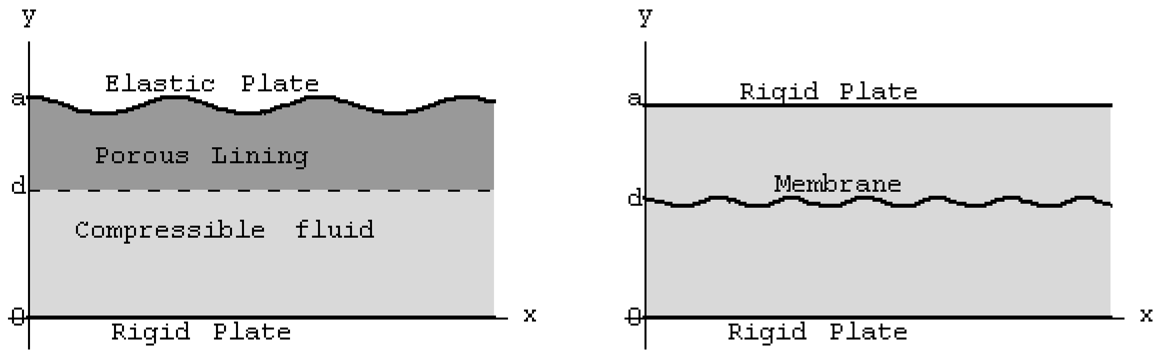

Figure 5: The xy-cross-sections for the lined 3-D duct and the 3-D drumlike silencer.

Consider, for example, the situation whereby a porous lining is inserted into the 3-D duct described in section 3. Suppose that the lining occupies the region $d \le y \le a$, $-b \le z \le b$, $-\infty < x < \infty$ where $d<a$, then the xy- cross-section of the duct is shown in figure 5. The porous

material is modelled as a fluid with complex density, ρ_ℓ , and propagation coefficient , Γ. These complex quantities are evaluated using the empirical formulae:

$$\Gamma = 1 + ia_1\xi^{a_2} + a_3\xi^{a_4} \quad \text{and} \quad \beta = \frac{\rho_\ell}{\rho_a} = \Gamma(1 + a_5\xi^{a_6} - ia_7\xi^{a_8}). \tag{13}$$

where $\xi = \rho_a f / \sigma$ in which f is the frequency, σ is the flow resistivity and $a_1 - a_8$ are constants the values of which depend on the porous material, [2,5]. Clearly, the unlined duct is retrieved on setting $\Gamma = \beta = 1$.

The eigenfunctions for this class of 2-D sub-system, [4], are given by:

$$Y_n(y) = \begin{cases} Y_{1n}(y), & 0 \le y < d \\ Y_{2n}(y), & d \le y \le a \end{cases} \tag{14}$$

where

$$Y_{1n}(y) = \cosh(\gamma_n y), \tag{15}$$

and

$$Y_{2n}(y) = \gamma_n \sinh(\gamma_n d)\frac{\sinh[\lambda_n(y-d)]}{\lambda_n} + \frac{1}{\beta}\cosh(\gamma_n d)\cosh[\lambda_n(y-d)]. \tag{16}$$

with $\lambda_n = (\gamma_n^2 + 1 - \Gamma^2)^{1/2}$. Note that $Y'_{1m}(d) = Y'_{2m}(d)$ implying continuity of normal velocity at the interface between the compressible fluid and the porous material. Likewise, $Y_{1m}(d) = \beta Y_{2m}(d)$ ensuring continuity of pressure, and $Y'_{1m}(0) = 0$ which is consistent with the rigid base of the 2-D duct at *y=0*.

For the case in hand, γ_m, $m = 0,1,2,\ldots$ are defined to be the roots of $Q(\gamma) = 0$ where

$$Q(\gamma) = ((\gamma^2 + 1)^2 - \mu^4)Y'_{2n}(a) - \alpha Y_{2n}(a). \tag{17}$$

Note also that $Y_m(y)$, $m = 0,1,2,\ldots$ are linearly dependent and satisfy the orthogonality relation

$$\alpha\int_0^d Y_{1m}Y_{1j}\,dy + \alpha\beta\int_d^a Y_{2m}Y_{2j}\,dy = C_m\delta_{mj} - \beta(\gamma_j^2 + \gamma_m^2 + 2)Y'_{2m}(a)Y'_{2j}(a) \tag{18}$$

where C_m is defined by

$$C_m = \beta\frac{Y'_{2n}(a)}{2\gamma_m}\frac{d}{d\gamma}Q(\gamma)\bigg|_{\gamma=\gamma_m}. \tag{19}$$

The correct eigenfunctions and characteristic equation for the lined 3-D duct with one flexible wall are now given by equations (7) and (8) in conjunction with (14) and (19).

Other 3-D ducts can be handled in the same way. For example, equations (7) and (8) together with the 2-D eigenfunctions discussed by Lawrie and Guled, [4], yield the waveforms and characteristic equation for a 3-D duct with an internal membrane lying along $y = d$, $-b \le z \le b, -\infty < x < \infty$, where $d < a$ (see figure 5 for the xy-cross-section). In this case, since the flexible surface lies along $y = d$, the derivatives $Y_m'(d)$ will occur in (7) and (8) as opposed to $Y_m'(a)$. This latter duct is an important component of the drumlike silencer, [3].

6 Conclusions

The eigenfunctions for 3-D ducts with rectangular cross-section and one flexible wall have been explored, and the analysis of Lawrie, [6], extended to include porous linings and other internal structures. This class of problem has direct relevance to the HVAC industry, in which ducting systems are commonly constructed using sections of unlined duct together with silencing components. The 3-D eigenfunctions considered herein satisfy orthogonality relations equivalent to equations (4) and (18). Thus, the analytic tools are in place to construct mode-matching solutions to benchmark problems that closely model real ducting systems.

7 References

1. H. Besserer & P. Malischewsky, “Mode series expansions at vertical boundaries in elastic waveguides”, Wave Motion, **39**, 41-59, (2004).
2. M.E. Delany & E.N. Bazley, “Acoustic properties of fibrous materials”, Applied Acoustic, **3**, 105-116 (1970).
3. L. Huang & Y.S. Choy, “Vibroacoustics of three-dimensional drum silencer”", J. Acoust. Soc. Am., **118**, 2313-2320, (2005).
4. I.M.M. Guled, “Acoustic transmission: waveguides with scattering or dissipative components”, Thesis, Brunel University, U.K., (2003).
5. R. Kirby & A. Cummings A, “Prediction of the bulk acoustic properties of fibrous materials at low frequencies”, Applied Acoustic, **56**, 101-125, (1998).
6. J.B. Lawrie, “Orthogonality relations for fluid-structural waves in a 3-D rectangular duct with flexible walls”, Proc. R. Soc. **A.**, **465**, 2347-2367, (2009).
7. J.B. Lawrie, & I.M.M Guled, “On tuning a reactive silencer by varying the position of an internal membrane.” Jl Acoust. Soc. Am, **120**, 780-790, (2006).
8. J.B. Lawrie & R. Kirby, "Mode-matching without root-finding: application to a dissipative silencer.” Jl. Acoust. Soc. Am., **119**, 2050-2061 (2006).
9. V. Martin, A. Cummings & C. Gronier, ``Discrimination of coupled structural/acoustical duct modes by active control: principles and experimental results", J. Sound Vib., **274**, 583-603, (2004).